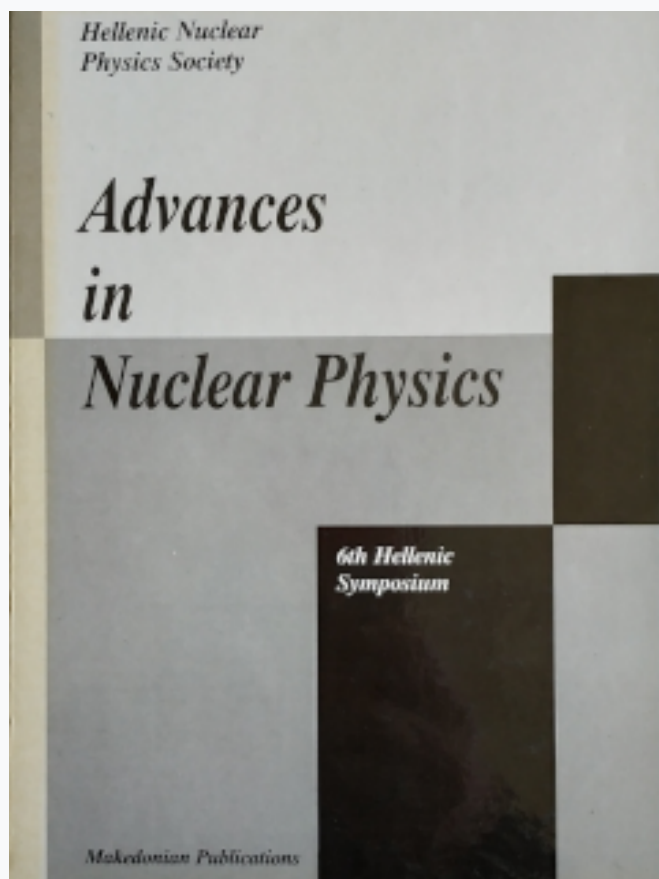


## HNPS Advances in Nuclear Physics

Vol 6 (1995)

HNPS1995



**Double-, energy-, angle- differential and total yield cross section data of  $^{58}\text{Ni}(\text{n},\text{a})^{55}\text{Fe}$  reaction**

*C. Tsabarlis, R. Vlastou, C. T. Papadopoulos, C. A. Kalfas, E. Wattecamp, G. Rollin*

doi: [10.12681/hnps.2926](https://doi.org/10.12681/hnps.2926)

### To cite this article:

Tsabarlis, C., Vlastou, R., Papadopoulos, C. T., Kalfas, C. A., Wattecamp, E., & Rollin, G. (2020). Double-, energy-, angle- differential and total yield cross section data of  $^{58}\text{Ni}(\text{n},\text{a})^{55}\text{Fe}$  reaction. *HNPS Advances in Nuclear Physics*, 6, 176–186. <https://doi.org/10.12681/hnps.2926>

# Double-, energy-, angle- differential and total yield cross section data of $^{58}\text{Ni}(\text{n},\alpha)^{55}\text{Fe}$ reaction

C. Tsabarlis, <sup>a</sup> R.Vlastou, <sup>a</sup> C.T.Papadopoulos, <sup>a</sup> C.A. Kalfas, <sup>b</sup> E. Wattecamp, <sup>c</sup> and G.Rollin <sup>c</sup>

<sup>a</sup> *National Technical University of Athens 15773 Athens, Greece*

<sup>b</sup> *NCSR Demokritos, Institute of Nuclear Physics 15310 Agia Paraskevi, Athens, Greece*

<sup>c</sup> *CEC JRC IRMM Retiesweg, B-2440 Geel Belgium*

---

## Abstract

The double-, energy-, angle- differential cross section data, and the total yield of  $^{58}\text{Ni}(\text{n},\alpha)^{55}\text{Fe}$  reaction is investigated in the neutron energy range between 2 and 9 MeV. The measurements were performed with the prompt detection method, detecting the alpha particles of the reaction with a multitelescope consisted of five  $\Delta\text{E}-\Delta\text{E}-\text{E}$  telescopes, placed at angles 14, 51, 79, 109 and 141 degrees relative to the neutron beam direction. The normalisation to the absolute units was made using the known total yield of the reference reactions  $^{27}\text{Al}(\text{n},\alpha)^{24}\text{Na}$  and  $^{58}\text{Ni}(\text{n},\text{p})^{58}\text{Co}$ . The cross section measurements were compared with previous measurements and with theoretical calculations performed with the STAPRE-H [1-4] code.

---

## 1 Introduction

The neutrons produced in the fusion reactors induce various endothermic or exothermic nuclear reactions, leading the nuclei to different excited levels. These interactions between neutrons and structural materials of the reactors, are characterised by the nuclear cross section, the angular and energy distribution of the emitted particles, the discrete and the continuous states of the nuclei. These data have to be known for both theoretical study of nuclear reaction and research in the field of the reactor technology. In this work the cross section measurements, for the  $^{58}\text{Ni}(\text{n},\alpha)^{55}\text{Fe}$  reaction performed with the prompt technique detecting the outgoing alpha particles, are presented.

## 2 Experimental setup-Data analysis

A monochromatic neutron beam was used in the neutron energy range between 2.0 and 9.0 MeV. The neutrons were produced via the D(d,n) and T(p,n) reactions. The incident particles of the above reactions loose a part of their energy due to the thickness of the target and according to the kinematics of the reactions a neutron spectrum is produced. The neutron spectra produced with the reactions D(d,n) and T(p,n) were simulated using the codes NUMAR [9] and NEUT [10]. The detection of the outgoing charged particles was performed by using the multitelescope [5, 6, 7, 8], shown in Fig. 1. Basically, the outgoing particles are detected from five telescopes which are placed at 14, 51, 79, 109 and 141 degrees relative to the neutron beam. Each telescope consists of surface barrier detector and two proportional counters ( $\Delta E$ - $\Delta E$ -E). The proportional counters consist from two anode planes and four cathode planes of wires on each side of the sample measuring the energy loss (E) of the particles. The rest energy (E) is measured by surface barrier detectors of  $400 \text{ mm}^2$  and either 100 or 1000  $\mu\text{m}$  thickness. An analytical study has been made for the gas pressure and high voltage for the optimum operation of the multitelescope [8]. In the middle of the multitelescope three samples and a source were placed : the sample of the reaction which has to be studied ( $^{58}\text{Ni}$ ), the sample of the reference reaction ( $^{58}\text{Ni}$  or  $^{27}\text{Al}$ ), the sample for the background measurement (Ta) and the  $^{241}\text{Am}$  source for the energy and efficiency calibration of the telescopes.

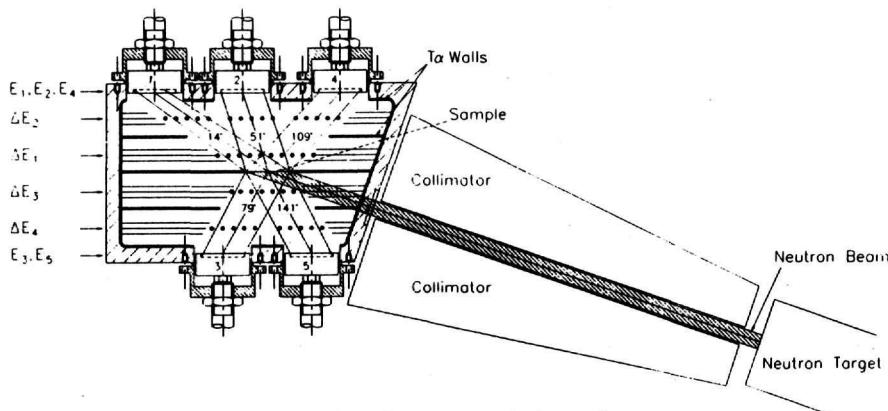


Fig 1. The multitelescope and the collimator

One of the main problems, for the performance of these type of measurements with the multitelescope, is the background of the particles produced from the interaction between the neutrons with the various materials of the multitelescope. In order to reduce the background of the measurements the multitelescope was constructed from Ta because the cross section of the reaction  $\text{Ta}(n,p)$  and  $\text{Ta}(n,\alpha)$  is very small ( $\sim 1 \text{ mbarn}$ ). A large proportion of

the background is due to the particles (alphas or protons), produced from the material (Si) of the surface barrier detector via the reactions  $\text{Si}(\text{n},\text{p})$  and  $\text{Si}(\text{n},\alpha)$ . An analytical study was made for the determination of the optimum length of the collimator [8] (21 cm) in order to reduce the ratio foreground - background.

A Ta sample was placed in the multitelescope for the background measurement. The background sample position was not left void because the background particles could pass from one part of the multitelescope to the other, therewith increasing the background. During the foreground-background measurements a systematic and continuous control was made for determination of the optimum conditions of the experiment.

The foreground and background spectra for the reactions  $^{58}\text{Ni}(\text{n},\alpha)$ ,  $^{58}\text{Ni}(\text{n},\text{p})$  and  $^{27}\text{Al}(\text{n},\alpha)$ , are shown in the Fig.2. The energy spectra of Ni, Al and Ta are collected for equal neutron fluences. The measurement for the alpha emission lasted 16h and for the proton emission 5h. The neutron energy was 8 MeV. The ratio of the foreground to background measurement was 3.5 for the  $^{58}\text{Ni}(\text{n},\alpha)$ , 4.8 for the  $^{58}\text{Ni}(\text{n},\text{p})$  and 2.1 for the  $^{27}\text{Al}(\text{n},\alpha)$  reactions respectively.

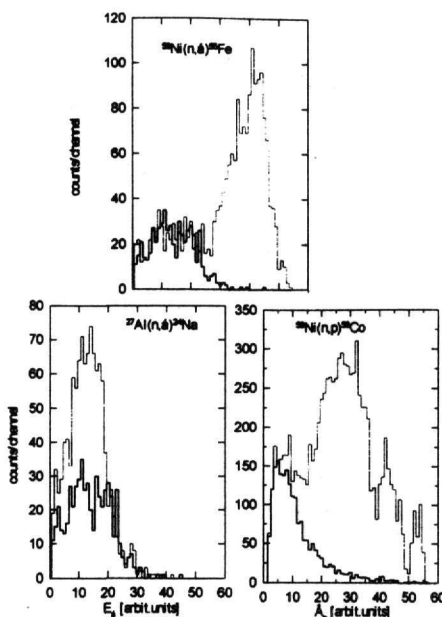


Fig. 2. Foreground (thin line) and background (thick line) spectra of the reactions  $^{58}\text{Ni}(\text{n},\alpha)$ ,  $^{58}\text{Ni}(\text{n},\text{p})$  and  $^{27}\text{Al}(\text{n},\alpha)$ .

So, a single telescope provides a proton or an alpha particle energy spectrum under a certain angle in relative units. By integration over all energies one deduces the angular distribution of the yield of protons or alphas for unitary

neutron fluence. These distributions are fitted by Legendre polynomials and the integration over  $4\pi$  sr is normalized to the known reference total yield values of the reactions  $^{27}\text{Al}(\text{n},\alpha)$  and  $^{58}\text{Ni}(\text{n},\text{p})$ .

The proton and alpha particle energy spectra are corrected for energy loss in the sample and in the telescope gas by an iterative unfolding procedure [8]. This effect becomes very strong when the emitted particles of the reaction are alphas. The calculations were performed with the CORRECTION.PRO programme and a detailed description as well as some results, are given earlier [8].

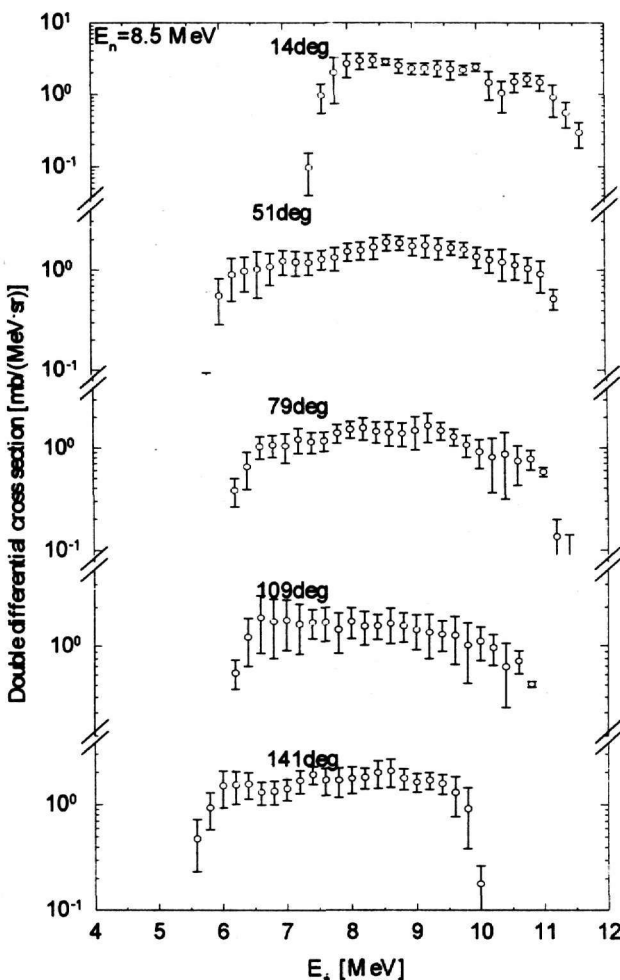


Fig 3 The measured double differential cross section data of the  $^{58}\text{Ni}(\text{n},\alpha)$  reaction at 8.5 MeV.

### 3 Cross section results

The double differential cross section of the reaction  $^{58}\text{Ni}(\text{n},\alpha)$  was measured at 6.5, 7.5, 8.0 and 9.0 MeV neutron energy. The normalisation was made with two reference reactions for which the absolute total yield is well known [10, 11]:  $^{27}\text{Al}(\text{n},\alpha)$  at 8.0, 9.0 MeV neutron energy and the  $^{58}\text{Ni}(\text{n},\text{p})$  reaction at 5.0, 7.5 and 8.5 MeV. At 6.5 MeV neutron energy the measured data were normalised with both reference reactions in order to check, if there is any discrepancy between the two results. The measured data in absolute units (mbarn/(MeV.sr)) for 8.0 MeV neutron energy are shown in the Fig. 3. At this neutron energy the alpha particles are emitted in the continuous region of the daughter nucleus  $^{55}\text{Fe}$ . This effect was expectable due to the fact that the level density is increasing exponentially as a function of the excitation energy. This increase has as a result the rise of the emission probability of the alpha particles in high energies. The discrete levels could not be observed for this reaction because the excitation energy of the compound nucleus was large (for example at  $E_{\text{n}}=8.0$  MeV  $\Rightarrow E^{\text{com}}=16.8$  MeV).

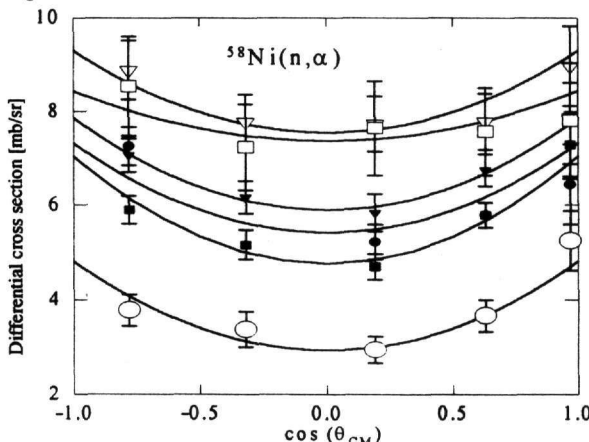


Fig.4 Measured angular distributions and Legendre polynomial fits of the  $^{58}\text{Ni}(\text{n},\alpha)$  reaction at the neutron energies [MeV]:  $\circ$  5.0,  $\blacksquare$  6.5,  $\bullet$  7.5,  $\nabla$  8.0,  $\blacktriangledown$  8.5,  $\square$  9.0

The angle-differential cross section can be extracted from the integration of the double differential cross section over the energy of the alpha particles. The measured values of the angular distribution with their uncertainties are shown in Fig 4. The data were parametrized by using the function  $f = a + 0.5b(3\cos^2\theta - 1)$ , which is the sum of the zero and the second order Legendre polynomials. This parametrization gives the integration of the data over  $4\pi$  sr and shows also the symmetry of the angular distribution around 90 degrees. The curve fits very well the experimental values within their uncertainties (see Fig 4). This symmetric distribution of the emitted alpha particles gives the information that the  $^{58}\text{Ni}(\text{n},\alpha)$  reaction proceeds via the compound

nucleus mechanism. The symmetric distribution is derived by the statistical model which is used to describe the interaction between the neutron and the  $^{58}\text{Ni}$  nucleus for the creation of the compound nucleus.

The energy-differential cross section can be extracted by integrating of the double differential cross section over the total emission angle ( $4\pi$  steradian). The experimental data of  $^{58}\text{Ni}(\text{n},\alpha)$  at 8.5 MeV energy are given in Fig. 5. It is observed that the energy distribution of the emitted alpha particles in this neutron energy is continuous. This is expected since at this neutron energy the energy of the compound nucleus  $^{59}\text{Ni}$  is relatively high (17.1 MeV) and the deexcitation of the compound nucleus will proceed via the high energetic nuclear states of the daughter nucleus  $^{55}\text{Fe}$ .

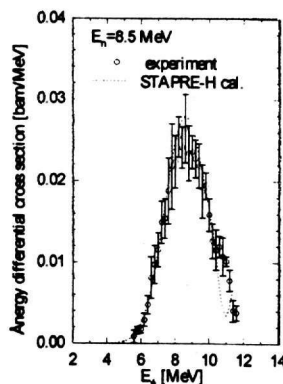


Fig 5 The energy-differential cross section data of the  $^{58}\text{Ni}(\text{n},\alpha)$  reaction at 8.5 MeV neutron energy.

The total yield of the alpha particle production taken by integrating the double differential cross section over the emission angle and the emission energy. The results with their uncertainties for this integration are presented in the Fig. 6. In addition to these data, experimental data from previous measurements are also presented. It is obvious that some of the previous measured values are in a big discrepancy (maximum 40%) due to the fact that a well known reference  $(\text{n},\alpha)$  reaction is missing and a neutron fluence measurement can not be accurate. The experimental values of this work agree with the data of works 11, 12, 13 and 14. The data from the work 11 are in a very good agreement for all neutron energies except the 8 MeV one. Both measurements were performed with the same detection device but the normalisation in the work 11 was made relative to the reference reaction  $\text{H}(\text{n},\text{n})\text{H}$ . The experimental values of this work improved the status of the cross section since the uncertainties fluctuating between 6 until 10%.

## 4 Nuclear model calculations

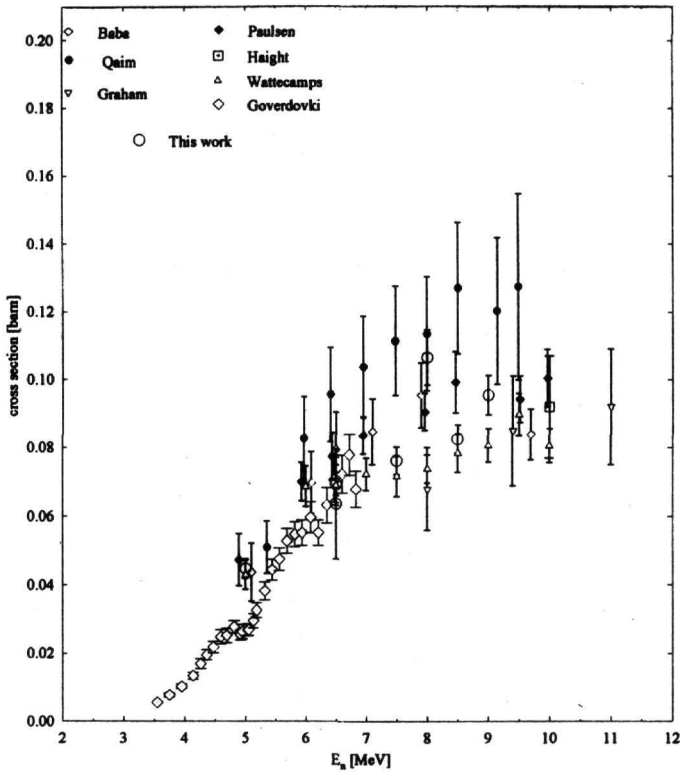


Fig 6 The excitation function of the  $^{58}\text{Ni}(\text{n},\alpha)$  reaction.

### 4.1 Theoretical Results

The energy differential cross section and the excitation function of the reaction  $^{58}\text{Ni}(\text{n},\alpha)$  are also calculated with the STAPRE-H [1, 2, 3, 4] code. The equilibrium emission is calculated with the Hauser - Feshbach model [15] and the pre-equilibrium emission with the Geometry-Dependent Hybrid Model [16]. The STAPRE-H code requires some fixed and some adjustable parameters for the cross section calculations. These parameters are given in the refs [7,8]. The cross section contribution according to the statistical and pre-equilibrium models as well as the experimental results of this work, are shown in Fig. 7.

The calculated cross section values agree very well with the experimental data except for the 8 MeV neutron energy where the theoretical value is 20% smaller than the experimental one (see Fig. 7). This discrepancy is due to a possible resonance, but it is difficult to maintain the existence of this resonance because

for this experiment a monoenergetic neutron beam is needed or practically a beam with energy spread of 70 keV. So, the measurement near 8 MeV and with an neutron energy spread of about 180 keV, could not show this resonance. It will be worthwhile to decrease the energy resolution of the neutron energy (that means longer radiation time) and to perform measurements near 8 MeV neutron energy.

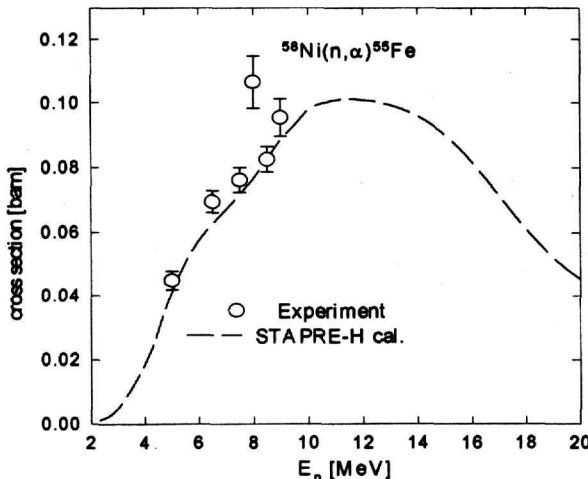


Fig 7 Measured and calculated cross section data of the  $^{58}\text{Ni}(\text{n},\alpha)$  reaction.

#### 4.2 Sensitivity Analysis

The model calculations are very sensitive to nuclear level density parameters and also to the optical potential parameters. The level density parameters have been studied in detail for all the nuclei used in the entrance and exit channels of the reaction [17]. So, a sensitivity analysis for the level density parameters was not necessary because the previous values [18] were not corresponding exactly to the nuclei which take place in the reaction  $^{58}\text{Ni}(\text{n},\alpha)$ , since they were known from a fitting curve made in a large atomic number interval ( $25 < A < 230$ ). The calculation using the values from the ref [18] gave higher (25%) results. The model calculations were also sensitive to the optical potential parameters, so an analysis was made using two different optical potentials for the alpha particles which are described in detail in the works [19,20]. The parameters from the optical potentials are given in table 1.

### Arthur - Young Potential

|                 |                     |              |                   |
|-----------------|---------------------|--------------|-------------------|
| Real Potential  | $V_r = 193 - 0.15E$ | $R_r = 1.37$ | $\alpha_r = 0.56$ |
| Complex surface | $W_s = 0$           |              |                   |
| potential       |                     |              |                   |
| Complex volume  | $W_v = 21 + 0.25E$  | $R_v = 1.37$ | $\alpha_v = 0.56$ |
| potential       |                     |              |                   |
| Spin - Orbit    | $V_{so} = 0$        |              |                   |
| potential       |                     |              |                   |

### McFadden - Satchler

|                 |              |              |                   |
|-----------------|--------------|--------------|-------------------|
| Real Potential  | $V_r = 185$  | $R_r = 1.40$ | $\alpha_r = 0.52$ |
| Complex surface | $W_s = 0$    | $R_v = 1.40$ |                   |
| potential       |              |              |                   |
| Complex volume  | $W_v = 25$   | $R_v = 1.40$ | $\alpha_v = 0.52$ |
| potential       |              |              |                   |
| Spin - Orbit    | $V_{so} = 0$ |              |                   |
| potential       |              |              |                   |

Table 1. The optical model parameters from the refs [19, 20].

The difference of the results using the two different sets of parameters is shown in Fig. 8. At low and high energies the cross section values of the reaction has almost the same value, while medium energies around 10 MeV the results, using the two different optical model parameters, show a discrepancy of 15%. The calculated values shown at Fig. 8 are produced only using the contribution from the statistical model.

## 5 Discussion

The measurement using the multitelescope provides in detail the emission of the outgoing particles of the reactions as a function of the emission energy, the emission angle as well as the incident neutron energy. A reference reaction was used in order to avoid an absolute measurement of the neutron fluence. A simple measurement of reaction rate ratios, for the  $^{58}\text{Ni}(n,\alpha)^{55}\text{Fe}$  reaction as well as for the reference reaction gives the cross section of the requested

reaction, since the cross section value of the reference reaction is well known from the literature. The normalization to the absolute units using the reference reactions  $^{27}\text{Al}(\text{n},\alpha)^{24}\text{Na}$  and  $^{58}\text{Ni}(\text{n},\text{p})^{58}\text{Co}$  is adequate but the latter is preferred since the cross section values are higher, the threshold of the reaction is low (~1 MeV) and the emitted particles have more energy.

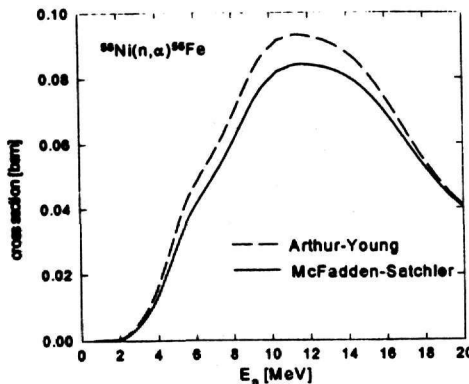


Fig 8 Calculated excitation functions of the  $^{58}\text{Ni}(\text{n},\alpha)$  reaction using two optical potentials.

The  $^{58}\text{Ni}(\text{n},\alpha)^{55}\text{Fe}$  reaction cross section data of this experiment globally confirm the lower data available in literature. The accuracy of this and other recent measurements may suggest the use of this reaction as a reference, but the level of accuracy expected remains questionable. The cross section value at 8 MeV neutron energy is almost 20% higher among all other available data in literature. A second measurement in this work confirmed our high value. Steep structures might exist in the excitation function and one ought to measure in small energy intervals (200 keV) with good neutron energy resolution (< 70 keV). The comparison of measured data with calculated cross section data obtained with the STAPRE-H code is satisfactory. The pre-equilibrium emission of the alpha particles is stronger at high neutron energies because the interaction time between the neutron with the  $^{58}\text{Ni}$  nucleus is small so, some alpha particles are emitted before the formation of the compound nucleus ( $^{59}\text{Ni}$ ), since the nuclear system (neutron +  $^{58}\text{Ni}$ ) can not reach the thermodynamic equilibrium.

## References

- [1] V. Avrigeanu, M. Avrigeanu and M. Ivasku, NEA Data Bank, IAEA 0971 pac.02- (1988).
- [2] O. Bersillon Report CEA-N-2227, CE, Bruyeres-le-Chatel(1981).

- [3] B. Strohmaier et al., Proceedings of the Course on Nuclear for Applications, Trieste, IAEA,-SRM-43, p.313(1980).
- [4] M. Blann, Report COO-3494-10(1973).
- [5] A. Paulsen, H. Liskien, F. Arnotte and R. Widera, Nucl. Sci. & Eng. 78, 337 (1981).
- [6] E. Wattecamps, H Liskien and F. Arnotte, Proc. Int. Conf. Nuclear Data for Scince and Technology, Antwerpen p.156 (1983).
- [7] C Tsabarlis, E.Wattecamps, G. Rollin and C. Papadopoulos, Nucl. Sci. & Eng. to be published.
- [8] C. Tsabarlis, Doctoral Thesis Study of (n,) and (n,p) reactions on the isotopes  $^{27}\text{Al}$ ,  $^{58}\text{Ni}$  and  $^{63}\text{Cu}$ , Athens, National Technical University.
- [9] A. Widera, Report GE/R/VG/65/81 (1981).
- [10] I. Birn, Report KFA-INC-IB-1/92 (1992).
- [11] E. Wattecamps, Proc. Int. Conf., Nuclear Data for Scince and Technology, Julich p.310 (1991).
- [12] S. L. Graham M. Ahmad, S. M. Grimes, H. Satyanarayana and S. K. Saraf, Nucl. Sci. Eng. 95, 60 (1987).
- [13] A. Goverdovski, V. A. Khryachkov, V. V. Ketleron, V. Mitrofanov, H. Vonach and R. C. Haight, Proc. Int. Conf. Nuclear Data for Scince and Technology, Gatlinburg (1994).
- [14] M. Baba, N. Ito, I. Matsuyama, S. Matsuyama, N. Hirakawa, S. Chiba, T. Fukahori, M. Mizumoto, K. Hasegawa and S. Meigo, Jour. Nucl. Sci. Tech. 31, 745 (1994).
- [15] W. Hauser and Feshbach, Phys. Rev. 87, 366 (1952).
- [16] M. Avrigeanu, V. Avrigeanu and M. Ivasku, Z. Phys. A 329, 177 (1998).
- [17] M. Ivasku, V. Avrigeanu and M. Avrigeanu, Rev. Roum. Phys. 32, 697 (1987).
- [18] W. Dilg et al., Nucl.Phys.A217, 269 (1973).
- [19] E. Arthur and Young, Report LA-8626-MS (ENDF-304), (1980)
- [20] Mac Fadden and G. Satchel, Nucl.Phys. A84, 177 (1996).